12th International Symposium on Turbulence and Shear Flow Phenomena (TSFP12)
Osaka, Japan (Online), July 19-22, 2022

INLINE COALESCENCE OF TWO BUBBLES ASCENDING IN A SHEAR-THINNING VISCOELASTIC LIQUID

Wenjun Yuan
School of Chemical Engineering and Technology
Xi'an Jiaotong University
Xi'an 710049, China
wenjun.yuan@xjtu.edu.cn

ABSTRACT

Direct numerical simulations (DNS) are performed to investigate the inline rise of a pair of three-dimensional (3D) air bubbles in a viscoelastic liquid using the volume-of-fluid (VOF) approach with an adaptive mesh refinement technique. The exponential Phan-Thien Tanner (PTT) model is employed as the non-linear viscoelastic constitutive equation for the liquid. The numerical model has been validated by comparisons with previously published results, including the terminal velocity jump discontinuity of an isolated bubble rising in a viscoelastic fluid. Focusing on the inline rising bubble pair in such a viscoelastic medium, we found that for pairs including a leading bubble and a trailing bubble, drafting-kissing scenario occurs before the bubble-bubble coalescence. The long-range repulsion and the short-range attraction due to fluid elasticity are critical to the bubble pair interactions. Interestingly, the squeezing flow near the growing bubble neck seems to delay the coalescence process. The capillary wave propagating down to the coalesced bubble tip together with the extensional flow behind the stretched bubble, determines the generation of satellite microdroplets along the tail of the coalesced bubble.

Introduction

The dynamics of buoyancy-driven bubbles in liquids are naturally and widely occurring in chemical industries, such as as bubble column reactors (Besagni *et al.*, 2018), heat exchangers (Singh *et al.*, 2019) and petroleum furnaces (Joshi *et al.*, 2008), to name a few. Over the last decades, the investigations of bubbly flows (Liao *et al.*, 2015) and rising bubble behaviors (Tripathi *et al.*, 2015; Li & Gupta, 2019) have been extensively carried out for Newtonian fluids. However, many solutions in practical applications with the likes of emulsions, slurries and polymer melts, are non-Newtonian fluids (Chhabra, 2010), i.e., their viscosities are dependent on the shear strain applied to the liquid and they exhibit viscoelasticity. Although there are a considerable amount of literature available on the bubbles rising in non-Newtonian liquids (Zenit & Feng, 2018), the hydrodynamic interactions and coalescence of an inline, or tandem bubble pair in viscoelastic liquids are seldom studied.

Using an arbitrary Lagrangian–Eulerian method, Vélez-Cordero *et al.* (2011) examined the hydrodynamic interaction between two bubbles rising for different initial alignments in shear-thinning power-law fluids, and reported that the wake formed behind a leading bubble attracts the trailing bubble. The shear-thinning effect was found to decrease the minimum coalescence height of bubbles (Jiang *et al.*, 2011; Sun *et al.*, 2017). Especially, Lin & Lin (2003) studied two inline oblate-cusped bubbles rising in a viscoelastic fluid using particle image analyzer, and noted that two approaching bubbles result in a circulating flow back to the trailing bubble. Frank *et al.* (2012) indicated that a viscoelasticity-dependent minimum height is required to induce the bubble coalescence. It was observed that the coalescence for a large leading bubble and a small trailing bubble coalescence is drastically promoted in comparison with than that of two-equal bubble coalescence (Lin & Lin, 2009). According to the recent theoretical work of Zilonova *et al.* (2019), the elasticity can resist the motion of bubbles in space, and the relaxation time of the viscoelastic medium significantly affects the bubbles' translational movement. According to our recent work of Yuan *et al.* (2021*a*), the fluid elasticity can resist the motion of bubbles in space, and the relaxation time of the viscoelastic medium significantly affects the bubbles' translational movement. Unfortunately, due to experimental limitations, the role of elasticity has not yet been clearly clarified in the hydrodynamic interactions of a bubble pair ascending in viscoelastic liquids.

Methodology

We consider the isothermal, incompressible viscoelastic two-phase flow. The basic equations for the mass conservation and momentum balance are as follows,

$$\nabla \cdot u = 0, \tag{1}$$

$$\rho \left[\frac{\partial u}{\partial t} + u \cdot \nabla u \right] = -\nabla p + \nabla \cdot \tau + f_s - f_g. \tag{2}$$

where u, ρ, t and p are the velocity vector, fluid density, time and pressure, respectively. τ is the extra-stress tensor. The source terms $f_g = g\rho j$ and $f_s = \sigma \delta_s \kappa n$ have been added on the right hand side of the momentum equation, denoting the gravitational force acting in the negative y direction and the surface tension force at the gas-liquid interface, respectively. σ is the interfacial tension coefficient, and j indicates the unit vector along the y axis direction. δ_s is the delta distribution function, and $\kappa = \nabla \cdot n$ is the interface curvature, wherein n is the unit normal at the gas-liquid interface pointing towards the surrounding liquid phase.

To simulate viscoelastic fluid flows, it is a common approach to split the total extra-stress tensor in a solvent contribution (τ_s) and a polymeric contribution (τ_p), $\tau = \tau_s + \tau_p$.

In order to have a closed set of equations, we use the constitutive equation presented by Phan-Thien & Tanner (1977) for the simulation of polymer solutions and melts. Therefore, the solvent and the polymeric stress tensors can be written as,

$$\tau_s = 2\eta_s D \tag{3}$$

$$f\left(\mathrm{tr}\left(\tau_p\right)\right)\tau_p + \lambda\widetilde{\tau_p} = 2\eta_p D \tag{4}$$

where η_s and η_p are the solvent viscosity and the polymeric viscosity, respectively. λ is the relaxation time. The deformation gradient tensor D is given by,

$$D = \frac{1}{2}\left[\nabla u + (\nabla u)^{\mathrm{T}}\right] \tag{5}$$

The Gordon-Schowalter derivative $\widetilde{\tau_p}$ is defined as:

$$\widetilde{\tau_p} = \frac{\partial \tau_p}{\partial t} + u\cdot\nabla\tau_p - \tau_p\cdot\nabla u - \nabla u^{\mathrm{T}}\cdot\tau_p + \zeta\left(\tau_p\cdot D + D\cdot\tau_p\right) \tag{6}$$

where $\zeta \in [0,2]$ is a constant model parameter that controls the amount of movement between the fluid polymeric chains. The polymeric extra-stress tensor is related with the conformation tensor A by,

$$\tau_p = \frac{\eta_p}{\lambda(1-\zeta)}(A - I) \tag{7}$$

For the function $f\left(\mathrm{tr}\left(\tau_p\right)\right)$, we use its exponential form given by Phan-Thien (1978),

$$f\left(\mathrm{tr}\left(\tau_p\right)\right) = \exp\left(\frac{\varepsilon\lambda}{\eta_p}\mathrm{tr}\left(\tau_p\right)\right) \tag{8}$$

with ε representing a parameter related to the elongational behaviour of the model.

Following our previous work Yuan *et al.* (2021*b*, 2020), we adopt the finite volume adaptive solver originally developed by Pimenta & Alves (2018). The volume-of-fluid (VOF) approach was used to represent the interface between the two phases Comminal *et al.* (2018). In particular, the simulations were stabilized by reformulating the viscoelastic constitutive equations with the log-conformation representation Fattal & Kupferman (2004) (LCR) and with both-sides diffusion Xue *et al.* (1995) (BSD) in the momentum equation.

In the log-conformation tensor methodology, a new tensor Θ is defined as the natural logarithm of the conformation tensor,

$$\Theta = \ln(A) = R\ln(\Lambda)R^{\mathrm{T}} \tag{9}$$

In Eq. 9, the conformation tensor was diagonalized ($A = R\Lambda R^{\mathrm{T}}$) because it is positive definite, where R is a matrix containing in its columns the eigenvectors of A and Λ is a matrix whose diagonal elements are the respective eigenvalues resulting from the decomposition of A. Eq. (4) written in terms of Θ becomes,

$$\frac{1}{\lambda}g(\Theta) = \frac{\partial\Theta}{\partial t} + u\cdot\nabla\Theta - (\Omega\Theta - \Omega\Theta) - 2B \tag{10}$$

where $g(\Theta)$ is a model-specific tensorial function depending on Θ. The tensor Ω is anti-symmetric and generates a pure rotation, while B is symmetric and generates a pure extension, which have been given by Fattal & Kupferman (2004). After solving Eq. 10, Θ is diagonalized in the form,

$$\Theta = R\Lambda^{\Theta}R^{\mathrm{T}} \tag{11}$$

and the conformation tensor is recovered by the inverse relation of Eq. 9,

$$A = \exp(\Theta) = R\exp\left(\Lambda^{\Theta}\right)R^{\mathrm{T}} \tag{12}$$

so that the polymeric extra-stress tensor can be computed from A (Eq. 7) and used in the momentum equation.

Validation

Fig. 1 shows the terminal mass centre rise velocity (U_b) of an isolated bubble as a function of its volume (V_b). Note that, both the coordinates are logarithmic. The obtained terminal rise velocities at different bubble volumes are quantitatively consistent with the experimental results (Pilz & Brenn, 2007) and simulation data (Niethammer *et al.*, 2019). Moreover, U_b slightly increases with V_b before the volume reaches a critical value $V_{b,crit}$. There is an abrupt increase of U_b at the critical bubble volume, corresponding to 40 mm^3 $<V_b<$50 mm^3 in our simulations. The value of $V_{b,crit}$ and the magnitude of the rise velocity jump are both in good agreements with the experimental results in Pilz & Brenn (2007). On the other hand, the velocity vector fields for subcritical (33 mm^3) and supercritical (51 mm^3) volume bubbles are shown in the inset diagrams. The negative wake behind the rising bubble with a cusped tail is visible for the supercritical state, which is also in accordance with the observations in the literature (Hassager, 1979). Hence, our 3D simulations have quantitatively predicted all the salient features for an isolated bubble rising in a viscoelastic fluid correctly (Yuan *et al.*, 2021*b*), paving the road for the present investigations on the hydrodynamic interaction and coalescence of two bubbles.

We define the above numerical simulations as Set A, which indicates that there exists a critical bubble volume at

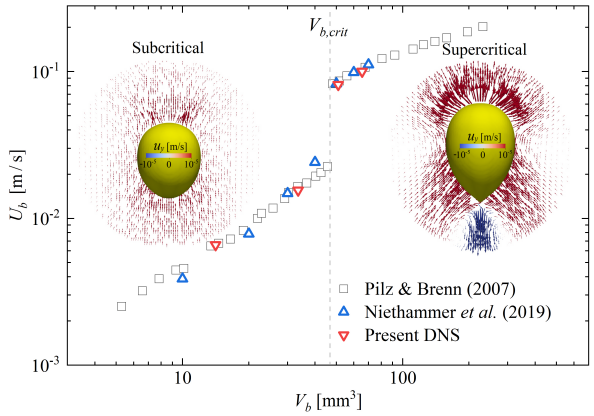

Figure 1: Terminal rise velocity as a function of the bubble volume for an isolated bubble rising in a viscoelastic fluid. Taken from (Yuan *et al.*, 2021*a*).

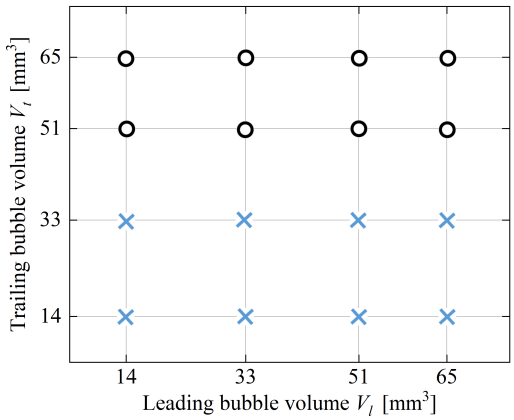

Figure 2: The behaviors of two bubbles rising inline with different volume configurations for initial separated distance $h_0 = 6$ mm. Note that, circles and crosses indicate the occurrence of coalescence and not, respectively.

Table 1: Rheological parameters for the polymer solution used in the simulations.

	β	λ[s]	γ[N/m]	η_s[Ns/m^2]	η_p[Ns/m^2]
Set A	0.02	0.207	0.076	0.031	1.511
Set B	0.02	0.207	0.038	0.002	0.098

which the bubble terminal velocity sharply increases in viscoelastic fluids. For such a liquid, different bubble volume configurations have been investigated for the leading and trailing bubbles with V_l and V_t = 14, 33, 51 and 65 mm^3 for initial separated distance h_0 = 6 mm. The results are given in Fig. 2, where the circles denote the cases in which the two inline bubbles can successfully coalesce during the rise process. We can see that the requirement of "a successful coalescence case" is that the trailing bubble is supercritical. However, it is noteworthy that the terminal rise velocity invariably increases with the bubble volume (Yuan *et al.*, 2021*b*). When the different size bubbles exchange the initial positions, it is believed that the local flow patterns in the neighbourhood of rising bubbles will make adjustment. For the different initial separated distance, the upward acceleration caused by the buoyancy may also affect the rise behaviors of the two co-axial bubbles.

In addition, to contrast the volume effects on the bubble dynamics in wide flow regimes, we also perform three-dimensional numerical simulations for different fluid physical properties. As the rise of an air bubble in viscoelastic fluids is a multi-physical phenomenon, we fix the polymer relaxation parameter λ and the viscosity ratio β in the simulations. The exponential PTT model for viscoelastic polymer solutions continues to be adapted and the extensibility parameter ε and the slip parameter ξ are set to constant 0.05 and 0, respectively. Another different set is obtained by changing the interfacial tension γ and the viscoelastic liquid viscosity η_B, as shown in Table 1. In the following, we present the inline rise of two bubbles for this Set B.

Results

Figs. 3 present the complex shapes of the inline rise of a trailing bubble and a leading bubble ($V_t = V_l$ = 51 mm^3). During the bubbles ascending, the leading one and trailing one get closer and closer to each other due to the buoyancy-driven upward flow. However, in contrast with the observation in (Yuan *et al.*, 2021*a*), the trailing bubble approaches the leading one and then coalesces with it. This attraction seems to be caused by the strong buoyancy force of the trailing bubble, which is acted on to generate the rapid initial acceleration (Yuan & Prosperetti, 1994).

Fig. 4 compares the detailed distributions of the polymeric stress components τ_{xx} and τ_{yy} in a vertical cutting plane during the bubble-bubble coalescence process at different time instants. For the short-range attraction in Figs. 4 before coalescence, τ_{xx} always has a positive large value between the two bubbles, while τ_{yy} is still modest. It is interesting to observe that as the bubbles are getting closer, the leading bubble bottom takes a remarkable bulge at t= 0.096 s rather than the flattened shape at the bubble lower hemisphere in Fig. 3 at t= 0.090 s. Moreover, it is obvious that at the lower raw of Fig. 4, the capillary wave propagates down from the growing coalesced neck to the bottom of the coalesced bubble. The comparison of these snapshots shows that the horizontal normal stress component τ_{xx} in the neighbourhood of the coalesced neck gradually fades away, and both the normal stress components τ_{xx} and τ_{yy} come to emerge near the coalesced bubble downstream pole. Recalling the results for an isolated bubble rising in viscoelastic fluids (Yuan *et al.*, 2021*b*), this indicates that polymeric stresses are squeezed in the small region near the bubble trailing end, which will further force the ejection of the satellite microdroplets. This is also the mechanism leading to the formation of a cusp shape with a tip at the supercritical bubble downstream pole, whereas the coalesced bubble has a larger volume, its tail is more likely to breakup with the propagating capillary wave.

In Fig. 5, the vertical velocity fields as well as the distribution of the trace of the natural logarithm of the conformation tensor Θ are presented in a vertical cutting plane through the bubble center. To reduce image duplication, the snapshots are visualized for the leading bubble and the trailing bubble during the coalescence process, corresponding to the bubble topology history in Fig. 4. From Figs. 5 , it is anticipated that the vertical fluid velocities around the coalesced bubble lower and upper hemispheres are enhanced by the coalescence, hence the coalesced bubble rises rapidly. For the instant before the coalescence in Fig. 5, the magnitudes of negative and positive vertical velocity contours are increased at the leading bubble bottom and at the trailing bubble top, respectively, providing evidence that the two bubbles attract each other and then aggregate. This is at variance with the inline coalescence between two bubbles in Newtonian flows (Chen *et al.*, 2011; Zhang *et al.*, 2018), that the bubble-bubble interaction is only determined by the influence of the leading bubble wake on the trailing bubble. Regardless of the downward propagation of the capillary wave in (Yuan *et al.*, 2021*a*), the liquid circulation inside the growing neck is strong, reflecting the radically changing of the velocity at the top and the bottom of the coalesced bubble.

As shown in the lower raw of Figs. 5, the large value regions of tr(Θ) exist in the narrow regions between the two bubbles before coalescence. This indicates that the polymer molecules tend to deform greatly as the two bubbles approach. The squeezed film of the viscoelastic liquid is significantly thicker than that in (Yuan *et al.*, 2021*a*), so that the short-range attraction is strong due to elasticity, related to the apparent bulges at the bottom of the leading bubble and at the top of the trailing bubble at t= 0.096 s. Owing to the fact that the large

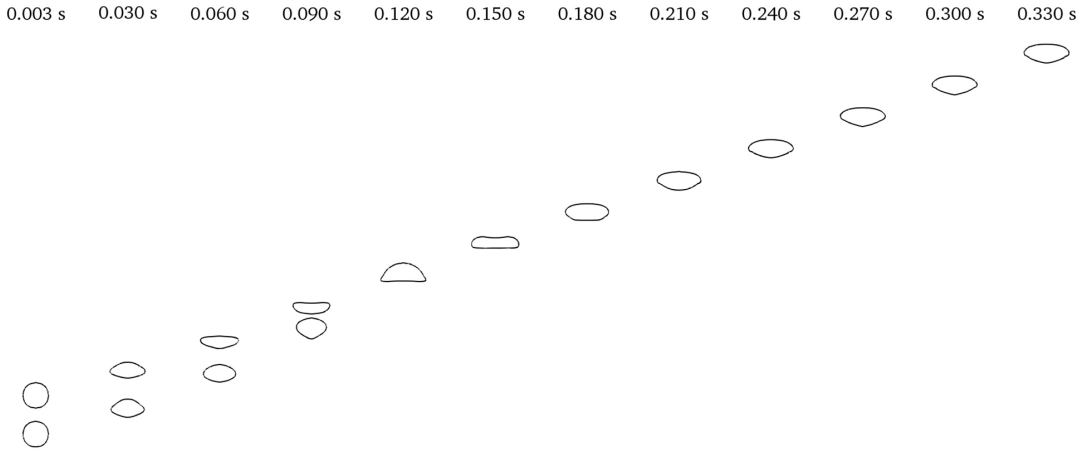

Figure 3: Complex shapes variation with time for the inline rise of a leading bubble and a trailing bubble in a viscoelastic fluid for Set B.

tr(Θ) occupies the region near the coalesced bubble neck, the polymer deformation seems to hinder the film drainage during the coalescence process (Dekee *et al.*, 1986). Conceivably, the elasticity in the liquid delays the coalescence, as a result of the squeezing flow in the film. The coalescence of the inline bubbles in this work is significantly different from the so-called drafting-kissing-tumbling scenario that occurs for bubble pairs in a Newtonian fluid and in a shear-thinning inelastic fluid (Chen *et al.*, 2011; Vélez-Cordero *et al.*, 2011).

Conclusions

To improve the understanding of bubble dynamics in non-Newtonian media, we have carried out direct numerical simulations (DNS) to explore the ascent of a pair of three-dimensional bubbles in a viscoelastic liquid. The adaptive mesh refinement approach is used to refine the mesh near the region of interest, and the exponential PTT model is employed to describe the shear-thinning viscoelasticity. On the basis of the good agreement between the present simulation results and experimental data by Pilz & Brenn (2007), we focus on the inline coalescence of a tailing bubble and a leading bubble. By probing the polymeric stresses and deformation, our results demonstrated that the short-range bubble-bubble attraction is strong due to the presence of elasticity, while the squeezing flow hinders the film drainage and delays the coalescence. In addition, the coalescence of large bubbles is more prevailing in highly elastic flows. The capillary wave propagating from the growing neck to the apex of the coalesced bubble and the extensional flow along the coalesced bubble tail, determine the generation of satellite microdroplets.

REFERENCES

Besagni, Giorgio, Inzoli, Fabio & Ziegenhein, Thomas 2018 Two-phase bubble columns: A comprehensive review. *ChemEngineering* **2** (2), 13.

Chen, RH, Tian, WX, Su, GH, Qiu, SZ, Ishiwatari, Yuki & Oka, Yoshiaki 2011 Numerical investigation on coalescence of bubble pairs rising in a stagnant liquid. *Chem. Eng. Sci.* **66** (21), 5055–5063.

Chhabra, Rajendra P 2010 Non-Newtonian fluids: an introduction. In *Rheology of complex fluids*, pp. 3–34. Springer.

Comminal, Raphaël, Pimenta, Francisco, Hattel, Jesper H, Alves, Manuel A & Spangenberg, Jon 2018 Numerical simulation of the planar extrudate swell of pseudoplastic and viscoelastic fluids with the streamfunction and the VOF methods. *J. Non-Newton Fluid Mech.* **252**, 1–18.

Dekee, D, Carreau, PJ & Mordarski, J 1986 Bubble velocity and coalescence in viscoelastic liquids. *Chem. Eng. Sci.* **41** (9), 2273–2283.

Fattal, Raanan & Kupferman, Raz 2004 Constitutive laws for the matrix-logarithm of the conformation tensor. *J. Non-Newton Fluid Mech.* **123** (2-3), 281–285.

Frank, Xavier, Charpentier, Jean-Claude, Ma, Youguang, Midoux, Noël & Li, Huai Z 2012 A multiscale approach for modeling bubbles rising in non-Newtonian fluids. *Ind. Eng. Chem. Res.* **51** (4), 2084–2093.

Hassager, O. 1979 Negative wake behind bubbles in non-Newtonian liquids. *Nature* **279** (5712), 402–403.

Jiang, Shaokun, Ma, Youguang, Fan, Wenyuan, Yang, Ke & Li, Huaizhi 2011 Chaotic behavior of in-line bubbles rising with coalescences in non-Newtonian fluids: A multiscale analysis. *Korean J. Chem. Eng.* **28** (1), 56–63.

Joshi, Jyeshtharaj B, Pandit, Aniruddha B, Kataria, Kamal L, Kulkarni, Rohit P, Sawarkar, Ashish N, Tandon, Deepak, Ram, Yad & Kumar, Man Mohan 2008 Petroleum residue upgradation via visbreaking: A review. *Ind. Eng. Chem. Res.* **47** (23), 8960–8988.

Li, Weihua & Gupta, Nivedita R 2019 Buoyancy-driven motion of bubbles in the presence of soluble surfactants in a Newtonian fluid. *Ind. Eng. Chem. Res.* **58** (18), 7640–7649.

Liao, Yixiang, Rzehak, Roland, Lucas, Dirk & Krepper, Eckhard 2015 Baseline closure model for dispersed bubbly flow: Bubble coalescence and breakup. *Chem. Eng. Sci.* **122**, 336–349.

Lin, Tsao-Jen & Lin, Gen-Ming 2003 The mechanisms of bubble coalescence in a non-Newtonian fluid. *Can. J. Chem.* **81** (3-4), 476–482.

Lin, Tsao-Jen & Lin, Gen-Ming 2009 Mechanisms of in-line coalescence of two-unequal bubbles in a non-Newtonian fluid. *Chem. Eng. J.* **155** (3), 750–756.

Niethammer, Matthias, Brenn, Günter, Marschall, Holger & Bothe, Dieter 2019 An extended volume of fluid method and its application to single bubbles rising in a viscoelastic liquid. *J. Comput. Phys.* **387**, 326–355.

Phan-Thien, Nhan 1978 A nonlinear network viscoelastic model. *J. Rheol.* **22** (3), 259–283.

Phan-Thien, Nhan & Tanner, Roger I 1977 A new constitutive equation derived from network theory. *J. Non-Newton Fluid*

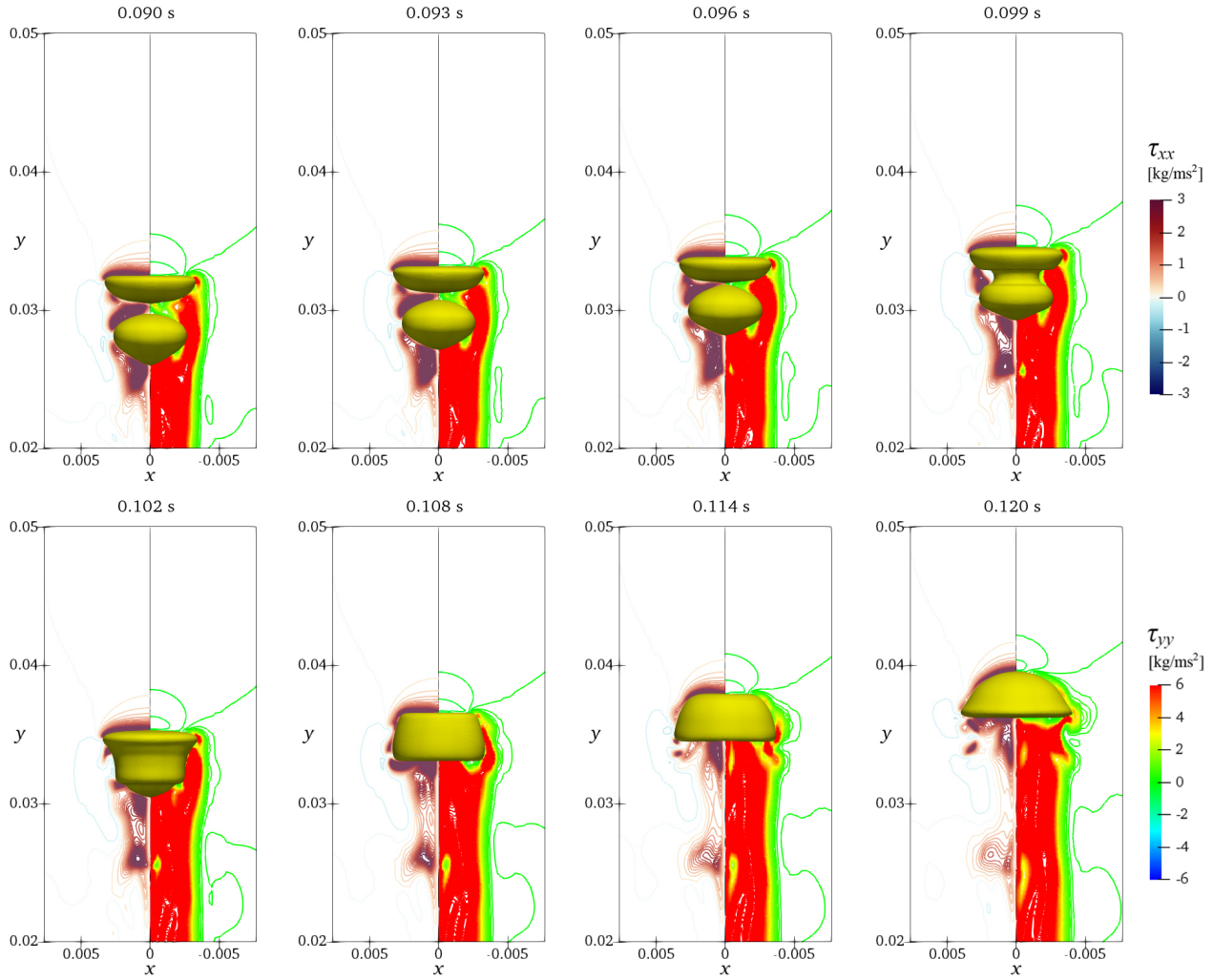

Figure 4: Distributions of the polymeric stress tensor components τ_{xx} (left) and τ_{yy} (right) in a vertical cutting plane through the centre of the rising bubbles during the inline coalescence process.

Mech. **2** (4), 353–365.

Pilz, C. & Brenn, G. 2007 On the critical bubble volume at the rise velocity jump discontinuity in viscoelastic liquids. *J. Non-Newton Fluid Mech.* **145** (2-3), 124–138.

Pimenta, F & Alves, MA 2018 Rheotool. https://github.com/fppimenta/rheoTool.

Singh, Jogender, Montesinos-Castellanos, Alejandro & Nigam, Krishna DP 2019 Process intensification for compact and micro heat exchangers through innovative technologies: A review. *Ind. Eng. Chem. Res.* **58** (31), 13819–13847.

Sun, Wanpeng, Zhu, Chunying, Fu, Taotao, Yang, Hui, Ma, Youguang & Li, Huaizhi 2017 The minimum in-line coalescence height of bubbles in non-Newtonian fluid. *Int. J. Multiph. Flow* **92**, 161–170.

Tripathi, Manoj Kumar, Sahu, Kirti Chandra & Govindarajan, Rama 2015 Dynamics of an initially spherical bubble rising in quiescent liquid. *Nat. Commun.* **6** (1), 6268.

Vélez-Cordero, J Rodrigo, Sámano, Diego, Yue, Pengtao, Feng, James J & Zenit, Roberto 2011 Hydrodynamic interaction between a pair of bubbles ascending in shear-thinning inelastic fluids. *J. Non-Newton Fluid Mech.* **166** (1-2), 118–132.

Xue, S-C, Phan-Thien, N & Tanner, RI 1995 Numerical study of secondary flows of viscoelastic fluid in straight pipes by an implicit finite volume method. *J. Non-Newton Fluid Mech.* **59** (2-3), 191–213.

Yuan, H & Prosperetti, A 1994 On the in-line motion of two spherical bubbles in a viscous fluid. *J. Fluid Mech.* **278**, 325–349.

Yuan, Wenjun, Zhang, Mengqi, Khoo, Boo Cheong & Phan-Thien, Nhan 2020 Dynamics and deformation of a three-dimensional bubble rising in viscoelastic fluids. *J. Non-Newton Fluid Mech.* **285**, 104408.

Yuan, Wenjun, Zhang, Mengqi, Khoo, Boo Cheong & Phan-Thien, Nhan 2021*a* Hydrodynamic interaction and coalescence of two inline bubbles rising in a viscoelastic liquid. *Phys. Fluids* **33** (8), 083102.

Yuan, Wenjun, Zhang, Mengqi, Khoo, Boo Cheong & Phan-Thien, Nhan 2021*b* On peculiar behaviours at critical volumes of a three-dimensional bubble rising in viscoelastic fluids. *J. Non-Newton Fluid Mech.* **293**, 104568.

Zenit, R. & Feng, J.J. 2018 Hydrodynamic interactions among bubbles, drops, and particles in non-Newtonian liquids. *Annu. Rev. Fluid Mech.* **50**, 505–534.

Zhang, Yang, Chen, Ke, You, Yunxiang & Ren, Wei 2018 Coalescence of two initially spherical bubbles: Dual effect of liquid viscosity. *Int. J. Heat Fluid Flow* **72**, 61–72.

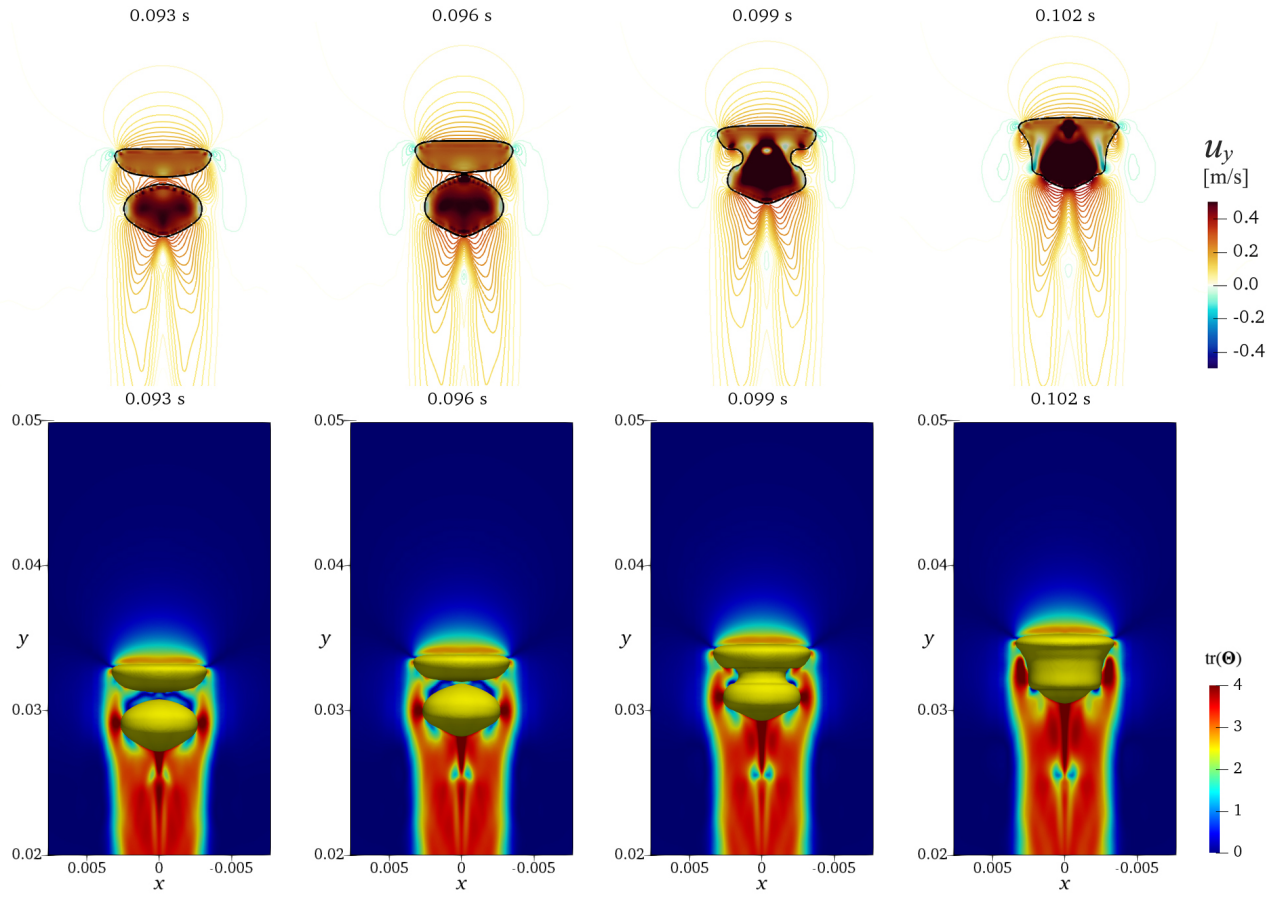

Figure 5: Vertical fluid velocity contours and distributions of the trace of the natural logarithm of the conformation tensor $\boldsymbol{\Theta}$ in a vertical cutting plane through the rising bubbles during the inline coalescence.

Zilonova, Ekaterina, Solovchuk, Maxim & Sheu, TWH 2019 Dynamics of bubble-bubble interactions experiencing viscoelastic drag. *Phys. Rev. E* **99** (2), 023109.